JCM
Journals.ASM.org

Isolation and Characterization of Porcine Epidemic Diarrhea Viruses Associated with the 2013 Disease Outbreak among Swine in the United States

Qi Chen,[a] Ganwu Li,[a] Judith Stasko,[b] Joseph T. Thomas,[a] Wendy R. Stensland,[a] Angela E. Pillatzki,[a] Phillip C. Gauger,[a] Kent J. Schwartz,[a] Darin Madson,[a] Kyoung-Jin Yoon,[a] Gregory W. Stevenson,[a] Eric R. Burrough,[a] Karen M. Harmon,[a] Rodger G. Main,[a] Jianqiang Zhang[a]

Department of Veterinary Diagnostic and Production Animal Medicine, College of Veterinary Medicine, Iowa State University, Ames, Iowa, USA[a]; Microscopy Services Unit, National Animal Disease Center, Agricultural Research Service, USDA, Ames, Iowa, USA[b]

Porcine epidemic diarrhea virus (PEDV) was detected in May 2013 for the first time in U.S. swine and has since caused significant economic loss. Obtaining a U.S. PEDV isolate that can grow efficiently in cell culture is critical for investigating pathogenesis and developing diagnostic assays and for vaccine development. An additional objective was to determine which gene(s) of PEDV is most suitable for studying the genetic relatedness of the virus. Here we describe two PEDV isolates (ISU13-19338E and ISU13-22038) successfully obtained from the small intestines of piglets from sow farms in Indiana and Iowa, respectively. The two isolates have been serially propagated in cell culture for over 30 passages and were characterized for the first 10 passages. Virus production in cell culture was confirmed by PEDV-specific real-time reverse-transcription PCR (RT-PCR), immunofluorescence assays, and electron microscopy. The infectious titers of the viruses during the first 10 passages ranged from 6×10^2 to 2×10^5 50% tissue culture infective doses ($TCID_{50}$)/ml. In addition, the full-length genome sequences of six viruses (ISU13-19338E homogenate, P3, and P9; ISU13-22038 homogenate, P3, and P9) were determined. Genetically, the two PEDV isolates were relatively stable during the first 10 passages in cell culture. Sequences were also compared to those of 4 additional U.S. PEDV strains and 23 non-U.S. strains. All U.S. PEDV strains were genetically closely related to each other (≥99.7% nucleotide identity) and were most genetically similar to Chinese strains reported in 2011 to 2012. Phylogenetic analyses using different genes of PEDV suggested that the full-length spike gene or the S1 portion is appropriate for sequencing to study the genetic relatedness of these viruses.

Porcine epidemic diarrhea (PED) was first observed in feeder pigs and fattening swine in England in 1971 (1). The causative agent, porcine epidemic diarrhea virus (PEDV), was identified in 1978 (2, 3). PEDV is an enveloped, single-stranded, positive-sense RNA virus belonging to the order *Nidovirale*, the family *Coronaviridae*, subfamily *Coronavirinae*, genus *Alphacoronavirus* (4). PEDV has a genome of approximately 28 kb and includes 5′ and 3′ untranslated regions (UTR) and 7 known open reading frames (ORFs) (5). ORF1a and ORF1b occupy the 5′ two-thirds of the genome and encode two replicase polyproteins (pp1a and pp1ab). Similar to other coronaviruses, expression of the pp1ab protein requires a −1 ribosomal frameshift during translation of the genomic RNA (6). The 3′-proximal one-third of the genome encodes four structural proteins, including spike (S), envelope (E), membrane (M), and nucleocapsid (N) proteins, and one hypothetical accessory protein encoded by ORF3 (5).

During the 1970s and 1990s, PEDV caused widespread epidemics in multiple swine-producing countries in Europe (2, 3, 7, 8). Since then, PED outbreaks have been rare in Europe, though occasional epidemics have been reported (9). In Asia, PED first occurred in Japan in 1982 (10), South Korea in 1993 (11), China (year unsure) (12, 13), and Thailand in 2009 (14). PED remains a major concern in Asian countries, particularly China. Since October 2010, a severe PED epizootic has been affecting pigs of all ages that is characterized by high mortality rates among suckling piglets in many provinces of China, resulting in tremendous economic losses (15–21).

PEDV was first detected in U.S. swine in May 2013 (22). Based on the USDA APHIS VS NVSL National Animal Health Laboratory Network (NAHLN) report, as of 28 September 2013, a total of 679 PEDV-positive swine cases (1,750 positive swine samples) from over 17 states have been diagnosed in the following age groups: 123 suckling, 94 nursery, 246 grower/finisher, 122 sow/boar, and 94 unknown ages (www.aasv.org). PED in U.S. swine is characterized by watery diarrhea, dehydration, variable vomiting, and high mortality in affected swine, particularly neonatal piglets (22). The clinical disease and lesions of PED are indistinguishable from those caused by transmissible gastroenteritis virus (TGEV), another *Alphacoronavirus*. As an acute, highly contagious, and devastating enteric disease, PED has caused significant economic loss to the U.S. swine industry, though the corresponding monetary values remain unknown.

Although a number of veterinary diagnostic laboratories quickly developed and launched PEDV-specific reverse-transcription PCR (RT-PCR) assays for accurate and rapid diagnosis of PEDV infection, more PEDV research is needed with regard to studying pathogenesis, evaluating the environmental stability of and effect of disinfectants on

Received 8 October 2013 **Accepted** 31 October 2013
Published ahead of print 6 November 2013
Editor: M. J. Loeffelholz
Address correspondence to Jianqiang Zhang, jqzhang@iastate.edu.

doi:10.1128/JCM.02820-13

the virus, developing and validating virological and serological diagnostic assays, and developing a live attenuated or inactivated vaccine for prevention and/or control of the disease. Obtaining a U.S. PEDV isolate that can grow efficiently in cell culture is critical for performing the aforementioned work. Attempts to grow PEDV in cell culture have proven difficult. Even if PEDV can be isolated from clinical samples, the virus may gradually lose infectivity upon further passages in cell culture. Here we report optimization of the procedures to isolate two U.S. PED viruses. At this time, the two isolates have been successfully serially propagated in cell cultures for over 30 passages, but only the first 10 passages of viruses have been characterized and reported in this study. In addition to characterizing the growth and titer of the virus during the serial passages in cell culture, we have also determined the entire genome sequences of viruses at selected passages to study their genetic stability. The sequences of the two U.S. PEDV isolates at different passages were compared to those of 4 additional U.S. PEDV strains whose sequences had been determined from clinical samples and of 23 PEDV strains collected outside the United States with entire genome sequences available to date. Phylogenetic analysis using different genes of PEDV was also performed to determine the gene(s) suitable for studying the genetic relatedness and molecular epidemiology.

MATERIALS AND METHODS

Clinical samples. Thirty-three feces and 17 intestinal homogenates that tested positive by a PEDV N gene-based real-time RT-PCR at the Iowa State University Veterinary Diagnostic Laboratory (ISU VDL) were selected for virus isolation (VI) attempts. Small-intestine tissues were used to generate a 10% (wt/vol) homogenate in Earle's balanced salt solution (Sigma-Aldrich, St. Louis, MO). The suspension was centrifuged at 4,200 × *g* for 10 min at 4°C. The supernatant was filtered through a 0.22-μm-pore-size filter and used as an inoculum for virus isolation. One-tenth gram of feces was suspended in 1 ml phosphate-buffered saline (PBS), vortexed for 5 min, and then centrifuged at 4,200 × *g* for 5 min. The supernatant was filtered through a 0.22-μm-pore-size filter and used as an inoculum for virus isolation.

PEDV N gene-based real-time RT-PCR. Viral RNA extraction was performed with 50 μl of small-intestine homogenates or virus isolates or 100 μl of processed feces using a MagMAX viral RNA isolation kit (Life Technologies, Carlsbad, CA) and a Kingfisher 96 instrument (Thermo Scientific, Waltham, MA) following the instructions of the manufacturers. Viral RNA was eluted into 90 μl of elution buffer. Real-time RT-PCR was performed on nucleic acid extracts using a Path-ID Multiplex One-Step RT-PCR kit (Life Technologies, Carlsbad, CA). The primers and probe targeting conserved regions of the PEDV nucleocapsid protein gene were as described by Kim et al. (23) with modifications to match a U.S. PEDV nucleotide sequence deposited in GenBank (accession no. KF272920). The real-time RT-PCRs were conducted on an ABI 7500 Fast instrument (Life Technologies, Carlsbad, CA) and the results analyzed by the system software.

Virus isolation, propagation, and titration. Virus isolation of PEDV was attempted on Vero cells (ATCC CCL-81) as previously described (24) with modifications. Vero cells were cultured and maintained in minimum essential medium (MEM) supplemented with 10% fetal bovine serum, 2 mM L-glutamine, 0.05 mg/ml gentamicin, 10 unit/ml penicillin, 10 μg/ml streptomycin, and 0.25 μg/ml amphotericin. Confluent Vero cells in 6-well plates were washed twice with the postinoculation medium and inoculated with 300 μl of sample and 100 μl of postinoculation medium. The postinoculation medium was MEM supplemented with tryptose phosphate broth (0.3%), yeast extract (0.02%), and trypsin 250 (5 μg/ml). After a 2-h incubation at 37°C with 5% CO_2, 3.6 ml postinoculation medium was added to each well. A similar inoculation was performed on Vero cells in 96-well plates (100 μl inoculum per well) for immunofluorescence staining. Inoculated cells (passage 0 [P0]) were incubated at 37°C with 5% CO_2. When a 70% cytopathic effect (CPE) developed, the plates were subjected to freeze-thaw once. The mixtures were centrifuged at 3,000 × *g* for 10 min at 4°C. The supernatants were harvested for further propagation or saved at −80°C. If no CPE was observed at 7 days postinoculation, the plates were frozen and thawed once and the supernatants were inoculated on new Vero cells for a second passage. Inoculated cells at each passage were also tested by an immunofluorescence assay (IFA) as described below. If CPE and IFA staining were negative after 4 passages, the virus isolation result was considered negative.

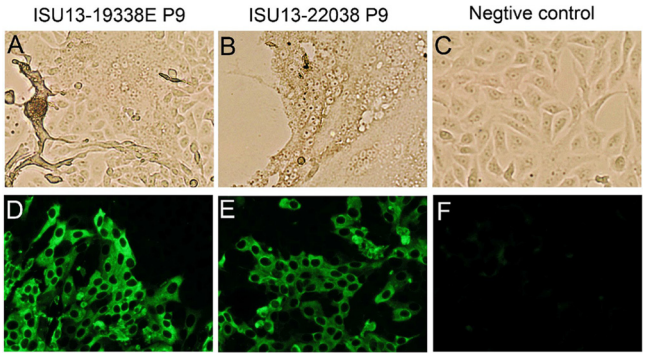

FIG 1 Cytopathic effects and IFAs of PEDV isolates in infected Vero cells. Vero cells were infected with PEDV 13-19338E P9 and PEDV 13-22038 P9 isolates. At 24 h postinfection, cytopathic effects were recorded (A, B, and C; ×160 magnification) and cells were examined by IFA using PEDV-specific monoclonal antibody (D, E, and F; ×100 magnification).

Virus titration was performed in 96-well plates with 10-fold serial dilutions performed in triplicate per dilution. After 5 days of inoculation, the plates were subjected to IFA staining and the virus titers determined according to the Reed and Muench method (25) and expressed as the 50% tissue culture infective dose ($TCID_{50}$)/ml.

Immunofluorescence assay. Inoculated cells in 96-well plates were fixed with 80% acetone, air dried, and incubated with 200× diluted mouse monoclonal antibody 6C8 (BioNote; Hwaseong-si, Gyeonggi-do, South Korea) specifically against PEDV (22) for 40 min followed by a 100× dilution of fluorescein-labeled goat anti-mouse IgG (KPL, Gaithersburg, MD). Cell staining was examined under a fluorescence microscope.

EM. Samples were prepared for negative-stain and thin-section examination by electron microscopy (EM) following previously described procedures (26) with modifications. The ISU13-22038 small-intestine homogenate was centrifuged at 4,200 × *g* for 10 min, and the supernatants were subjected to ultracentrifugation at 30,000 × *g* for 30 min to pellet the virus particles, which were then negatively stained with 2% phosphotungstic acid (PTA; pH 7.0) and examined with a FEI Tecnai G^2 BioTWIN electron microscope (FEI Co., Hillsboro, OR). Vero cells infected with the ISU13-22038 P3 virus isolate were trypsinized at 24 h postinfection and centrifuged at 800 × *g* for 5 min. The cell pellets were resuspended in 0.01 M PBS (pH 7.2 to 7.4) and centrifuged again at 800 × *g* for 5 min. The cell pellets were fixed with 2.5% glutaraldehyde–0.1 M sodium cacodylate. The cell pellets were postfixed in 1% osmium tetroxide for 90 min. The samples were dehydrated in an ascending ethanol series followed by propylene oxide and embedded in Eponate 12 resin (Ted Pella Inc., Redding, CA). Ultrathin sections were stained with uranyl acetate and lead citrate and examined with the FEI Tecnai G^2 BioTWIN electron microscope.

NGS. The sequences of the entire genome of PEDV in the original small-intestine homogenates as well as those of the P3 and P9 isolates were determined by next-generation sequencing (NGS) technology using an Illumina MiSeq platform. Total RNA from the homogenates and P3 and P9 PEDV isolates was extracted using a total RNA isolation kit (Norgen Biotek Corp., Niagara-on-the-Lake, Ontario, Canada). One hundred mi-

TABLE 1 Summary of two U.S. PEDV isolates during the first 10 passages in cell culture

Isolate and parameter	Origin of sample	Result[a]									
		Intestine homogenate	P0	P1	P2	P3	P4	P5	P6	P7	P8	P9
ISU13-19338	Indiana											
Cytopathic effect		N.A.	−	+	+	+	+	+	+	+	+	+
Real-time PCR C_T		17.0	16.0	15.2	15.4	16.3	14.0	15.8	16.9	15.1	11.2	11.7
Infectious titer ($\log_{10}$ $TCID_{50}$/ml)		N.D.	N.D.	N.D.	3.5	4.5	4.3	5.3	3.5	4.5	5.3	4.3
ISU13-22038	Iowa											
Cytopathic effect		N.A.	+	+	+	+	+	+	+	+	+	+
Real-time PCR C_T		16.0	17.2	13.8	12.2	14.8	18.0	13.9	10.0	14.3	14.6	13.8
Infectious titer ($\log_{10}$ $TCID_{50}$/ml)		N.D.	2.8	4.8	3.5	4.3	4.3	3.5	4.8	4.5	4.8	4.8

[a] N.A., not applicable; N.D., not done.

croliters of each sample was used to prepare the lysate, and the isolated RNA was eluted in 50 μl RNase-free water. The extracted RNA was quantified by the use of a Qubit 2.0 spectrophotometer (Life Technologies, Carlsbad, CA) to estimate concentrations and then stored at −80°C until use. The cDNA libraries were constructed from 100 ng of total RNA using a TruSeq Stranded total RNA sample preparation kit (Illumina, San Diego, CA) following the guidelines of the manufacturers. Multiplex libraries were prepared using barcoded primers and a median insert size of 340 bp. Libraries were analyzed for size distribution using a Bioanalyzer and quantified by quantitative RT-PCR using a Kapa library quantification kit (Kapa Biosystems, Boston, MA), and relative volumes were pooled accordingly. The pooled libraries were sequenced on an Illumina MiSeq platform with 150-bp end reads following standard Illumina protocols. An average of 0.8 Gb of sequence was produced per sample.

Sequences obtained by NGS technique were mapped to PEDV reference strain USA/Colorado/2013 (Genbank accession no. KF272920) or AH2012 (Genbank accession no. KC210145) using BWA software. Bases and single-nucleotide variants (SNVs) were called using the SAMtools "mpileup" command. Sites were filtered to avoid unreliable calls using the following criteria: (i) a minimum depth of 5 reads at each position, (ii) a

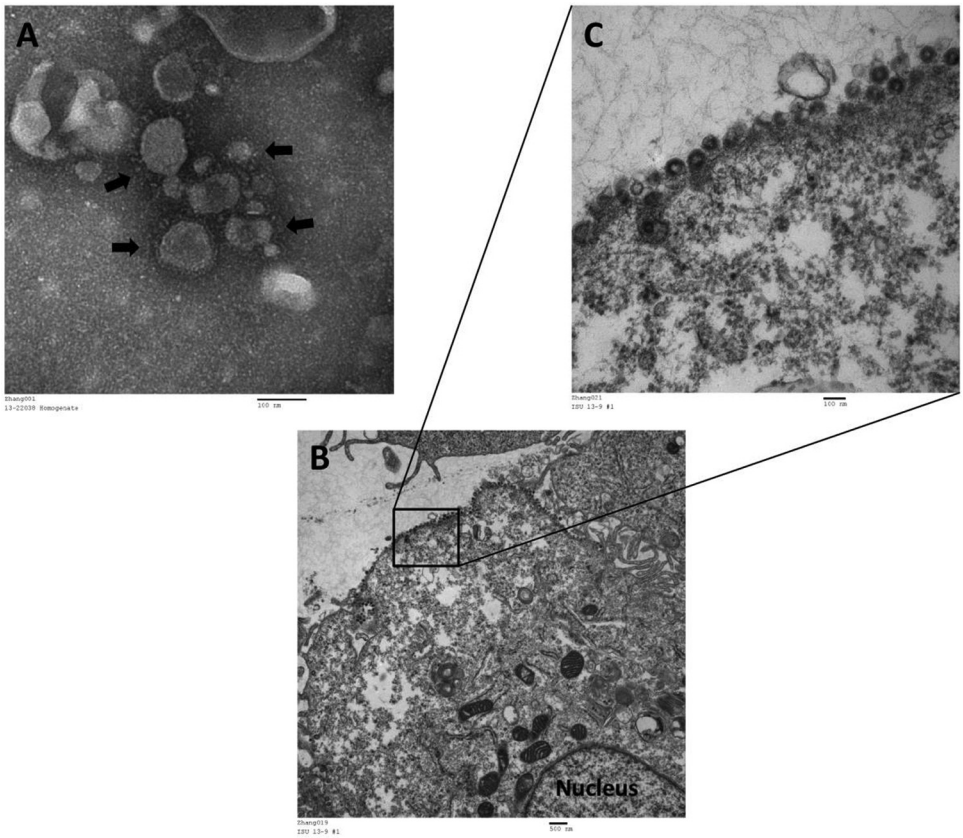

FIG 2 EM images on original homogenate and PEDV-infected Vero cells. (A) Negatively stained PEDV particles in the ISU13-22038 intestine homogenates. Some virus particles are shown by arrows. Crown-shaped spikes are visible. Bar = 100 nm. Magnification, ×150,000. (B) Thin section of Vero cells infected with ISU13-22038 P3 PEDV at 24 h postinfection. Bar = 500 nm. Magnification, ×11,000. (C) Enlarged image of the partial cytoplasm membrane showing accumulation of released virus particles. Bar = 100 nm. Magnification, ×68,000.

TABLE 2 Nucleotide and amino acid changes of PEDV isolates 13-19338E and 13-20338 during serial passages in cell culture

Virus	Genome region or ORF (nucleotide position[s])[a]	Encoded protein	Nucleotide in[a]:				Amino acid in[b]:			
			Position	Homogenate	P3	P9	Position	Homogenate	P3	P9
PEDV 13-19338E	5′ UTR (1–292)	None	–[c]	–	–	–				
	ORF1a (293–12646)	pp1a								
	ORF1ab (293–12616, 12616–20637)	pp1ab	1303	T	C	C				
			3519	C	T	T	1076	Ala	Val	Val
	S (20634–24794)	Spike	21403	A	A	G	257	Asn	Asn	Ser
			21756	C	T	T	375	Leu	Phe	Phe
	ORF3 (24794–25468)	Hypothetical protein 3	–	–	–	–	–	–	–	–
	E (25449–25679	Envelope	–	–	–	–	–	–	–	–
	M (25687–26367)	Membrane	–	–	–	–	–	–	–	–
	N (26379–27704)	Nucleocapsid	–	–	–	–	–	–	–	–
	3′ UTR (27705–28038)	None	–	–	–	–				
PEDV 13-22038	5′ UTR (1–292)	None	–	–	–	–				
	ORF1a (293–12646)	pp1a								
	ORF1ab (293–12616, 12616–20637)	pp1ab	10689	C	C	T	3466	Thr	Thr	Ile
	S (20634–24794)	Spike	21265	C	C	T	211	Thr	Thr	Ile
			21355	T	C	C	241	Val	Ala	Ala
	ORF3 (24794–25468)	Hypothetical protein 3	–	–	–	–	–	–	–	–
	E (25449–25679	Envelope	25616	G	G	T	56	Leu	Leu	Phe
	M (25687–26367)	Membrane	–	–	–	–	–	–	–	–
	N (26379–27704)	Nucleocapsid	–	–	–	–	–	–	–	–
	3′ UTR (27705–28038)	None	–	–	–	–				

[a] Nucleotides are numbered according to the PEDV 13-19338E sequences (GenBank accession no. KF650370).
[b] Only nonsynonymous mutations are shown, and silent mutations are not shown. Amino acids of replicase proteins are numbered according to their locations in the replicase polyprotein pp1ab. Amino acids of structural proteins are numbered according to their locations in the respective structural proteins.
[c] –, no nucleotide or amino acid change occurred.

minimum average base quality of 10, (iii) a minimum SNV quality of 25, and (iv) at least 85% of reads at the correct position to support the call as homozygous. The consensus sequences were generated by the VCFtools software package.

Sanger sequencing. The spike (S) gene sequences and partial ORF1b gene sequences of PEDV in the original homogenates and in P3 and P9 of both isolates were also determined by the traditional Sanger method to confirm the NGS results. The S gene was amplified in two fragments using a Qiagen One-Step RT-PCR kit (Qiagen, Valencia, CA). The first fragment was amplified using primers PEDV-S1F (5′-GTGGCTTTTCTAATCATTTGGTC-3′) and PEDV-S1R (5′-CTGGGTGAGTAATTGTTTACAACG-3′) under thermal cycler conditions of 50°C for 30 min, 95°C for 15 min, 40 cycles of 94°C for 30 s, 50°C for 30 s, and 72°C for 3.5 min, and 72°C for 10 min. The second fragment was amplified using primers PEDV-S2F (5′-GGCCAAGTCAAGATTGCACC-3′) and PEDV-S2R (5′-AGCTCCAACTCTTGGACAGC-3′) under thermal cycler conditions of 50°C for 30 min, 95°C for 15 min, 40 cycles of 94°C for 30 s, 53°C for 30 s, and 72°C for 2.5 min, and 72°C for 10 min. The partial ORF1b gene was amplified and sequenced using primers PEDV-19923F (5′-ACATGCGTGTGCTACATCTTGG-3′) and PEDV-20600R (5′-TGGCGTCATTATACGCACTAGC-3′) under thermal cycler conditions of 50°C for 30 min, 95°C for 15 min, 40 cycles of 94°C for 30 s, 54°C for 30 s, and 72°C for 1 min, and 72°C for 10 min. Sequence data were assembled and analyzed using the DNAStar Lasergene 11 Core Suite (DNAstar, Madison, WI).

Phylogenetic analysis. Phylogenetic analysis was performed using the nucleotide sequences of the six PEDV viruses from this study as well as four other U.S. PEDV strains (USA/Colorado/2013-KF272920 [27], IA2013-KF452322 [22], IN2013-KF452323 [22], and USA2013-019349-KF267450 [unpublished]) and 23 non-U.S. PEDV strains with entire genome sequences available in GenBank. Phylogenetic trees were constructed using the entire genome, the spike gene, the S1 portion (S gene nucleotides 1 to 2205, corresponding to amino acids 1 to 735) (28), the S2 portion (S gene nucleotides 2206 to 4152, corresponding to amino acids 736 to 1383) (28), a hypothetical protein gene (ORF3), the envelope (E) gene, the membrane (M) gene, and the nucleocapsid (N) gene sequences. The trees were constructed using the distance-based neighbor-joining method of MEGA5.2 software. Bootstrap analysis was carried out on 1,000 replicate data sets.

Nucleotide sequence accession numbers. The full-length genomic nucleotide sequences of the ISU13-19338E-IN homogenate, ISU13-19338E-IN P3, ISU13-19338E-IN P9, the ISU13-22038-IA homogenate, ISU13-22038-IA P3, and ISU13-22038-IA P9 were deposited in GenBank under accession numbers KF650370, KF650371, KF650372, KF650373, KF650374, and KF650375, respectively.

RESULTS

Virus isolation and characterization. Virus isolation was attempted on 33 PEDV-PCR-positive feces samples and 17 PEDV-PCR-positive intestine homogenates on Vero cells. Two PEDV isolates designated ISU13-19338E and ISU13-22038 were successfully obtained from the small intestines of piglets from sow farms in Indiana (collected on 16 May 2013) and Iowa (collected on 6 June 2013), respectively. Attempts at virus isolation from the remaining samples were unsuccessful. Cytotoxicity was observed in cells inoculated with several intestine samples and many of the fecal samples.

A distinct cytopathic effect (CPE), characterized by cell fusion, syncytium formation, and eventual cell detachment, was observed for ISU13-19338E from passage 1 (P1) and for ISU13-22038 from P0. In order to determine if the isolated viruses can be efficiently propagated and maintained in cell cultures, the two virus isolates were further serially passed in Vero cells for a total of 10 passages (P0 to P9). Prominent CPE was usually observed within 24 h post-inoculation during the propagation process. Examples of CPE and IFA images are shown in Fig. 1. Compared to the negative-control

Vero cells (Fig. 1C), the Vero cells infected with the ISU13-19338E P9 (Fig. 1A) and the ISU13-22038 P9 (Fig. 1B) isolates showed cell enlargement, obvious cell fusion, and syncytium formation. Virus growth was confirmed by IFA using 6C8, a PEDV-specific monoclonal antibody. The PEDV protein stained by the monoclonal antibody was distributed in the cytoplasm but not in the nucleus (Fig. 1D and E). During the first 10 serial passages, the infectious titers of both isolates ranged from 6×10^2 to 2×10^5 $TCID_{50}$/ml (Table 1). The level of viral genome or transcript in each passage for both isolates was also assessed by a PEDV N gene-based real-time RT-PCR, and the cycle threshold (C_T) values are shown in Table 1.

The PEDV particles in the small-intestine homogenates and in infected Vero cells were also examined by EM techniques. As shown in Fig. 2A, multiple virus particles with distinctive crown-shaped projections were visible in the 13-22038 small-intestine homogenates as examined by negative-staining EM. On thin sections of the Vero cells infected with the 13-22038 P3 isolate, masses of virus particles adhering to the cytoplasm membrane were observed at 24 h postinfection (Fig. 2B and C).

Genetic stability of PEDV isolates during serial passages in cell cultures. In order to determine if the two PEDV isolates are genetically stable during the first 10 serial passages in cell culture, the entire genomes of all six viruses (ISU13019338E homogenate, P3, and P9; ISU13022038 homogenate, P3, and P9) were sequenced using the NGS technology. Using the Colorado/2013 PEDV (GenBank accession no. KF272920) as the initial reference, the NGS reads of all six viruses were successfully assembled to obtain the entire genome sequences. All six PEDV viruses (ISU13019338E homogenate, P3, and P9; ISU13022038 homogenate, P3, and P9) have a genome 28,038 nucleotides in length. The genomic organization of all six PEDV viruses is similar to what was previously described (5, 27) and includes the 5′ UTR, ORF1a and ORF1b, S, ORF3, E, M, N, and 3′ UTR (Table 2). By alignment with other coronaviruses, the slippery sequence $_{12610}$TTTAAAC$_{12616}$ followed by sequences that form a putative pseudoknot structure was identified in PEDV genomes. Translation of the replicase pp1ab is assumed to occur by a −1 RNA-mediated ribosomal frameshift at the end of the slippery sequence; thus, the nucleotides encoding the pp1ab are predicted to be 293 to 12616 and 12616 to 20637 in the PEDV genomes (Table 2). The full-length S genes (about 4.1 kb) of all 6 PEDV viruses were also sequenced using the Sanger sequencing method, and the sequences were completely identical to those determined by the NGS for each virus (data not shown).

The entire genome sequences of PEDV from the homogenate and from the P3 and P9 cell cultures of the two isolated strains were compared, and the results are summarized in Table 2. Compared to the 13-19338E homogenate, 13-19338E P3 had acquired three nucleotide changes at positions 1303, 3519, and 21756, and 13-19338E P9 had acquired one additional nucleotide change at position 21403, at the whole-genome level. Three amino acid changes resulting from the nucleotide changes were located in the pp1ab (1 amino acid [aa]) and the spike protein (2 aa). Compared to the 13-22038 homogenate, 13-22038 P3 had acquired only one nucleotide change at position 21355, and 13-122038 P9 had acquired three additional nucleotide changes at positions 10689, 21265, and 25616, at the whole-genome level. Four amino acid changes resulting from the nucleotide changes were located in pp1ab (1 aa), the spike protein (2 aa), and the envelope protein (1

TABLE 3 Nucleotide differences and nucleotide identities of 33 PEDV strains with entire genome sequences available[a]

Strain	No. of nucleotide differences (% nucleotide identity)														
	13-19338E P3	13-19338E′9	13-22038 homogenate	13-22038 P3	13-22038 P9	Colorado2013_ KF272920	IA2013_ KF452322	IN2013_ KF452323	USA-13-019349_ KF267450	AH2012-KC210145	BJ-2011-1-JN825712	GD-B-JX088695	CH-ZMDZY_11_KC196276	JS-HZ2012-KC210147	SM98-GU937797	CV777_ AF353511
13-19338E homogenate	3 (99.9)	4 (99.9)	10 (99.9)	11 (99.9)	14 (99.9)	42 (99.8)	22 (99.9)	1 (99.9)	50 (99.8)	120 (99.5)	208 (99.2)	204 (99.2)	264 (99.0)	184 (99.3)	1,035 (96.3)	906 (96.7)
13-19338E P3		1 (99.9)	13 (99.9)	14 (99.9)	17 (99.9)	45 (99.8)	25 (99.9)	4 (99.9)	53 (99.8)	123 (99.5)	211 (99.2)	207 (99.2)	267 (99.0)	187 (99.3)	1,036 (96.3)	907 (96.7)
13-19338E P9			14 (99.9)	15 (99.9)	18 (99.9)	46 (99.8)	26 (99.9)	5 (99.9)	54 (99.7)	124 (99.5)	212 (99.2)	208 (99.2)	268 (99.0)	188 (99.3)	1,039 (96.2)	910 (96.7)
13-22038 homogenate				1 (99.9)	4 (99.9)	40 (99.8)	20 (99.9)	9 (99.9)	48 (99.8)	118 (99.5)	206 (99.2)	202 (99.2)	262 (99.0)	182 (99.3)	1,031 (96.3)	902 (96.7)
13-22038 P3					3 (99.9)	42 (99.8)	21 (99.9)	12 (99.9)	49 (99.8)	119 (99.5)	207 (99.2)	203 (99.2)	263 (99.0)	183 (99.3)	1,032 (96.3)	903 (96.7)
13-22038 P9						44 (99.8)	24 (99.9)	15 (99.9)	52 (99.8)	122 (99.5)	210 (99.2)	206 (99.2)	266 (99.0)	186 (99.3)	1,035 (96.3)	906 (96.7)
Colorado2013_ KF272920							53 (99.8)	43 (99.8)	15 (99.9)	138 (99.5)	196 (99.3)	192 (99.3)	276 (99.0)	172 (99.3)	1,034 (96.3)	905 (96.7)
IA2013_KF452322								22 (99.9)	55 (99.7)	128 (99.5)	218 (99.2)	214 (99.2)	274 (99.0)	194 (99.3)	1,022 (96.3)	893 (96.8)
IN2013_KF452323									49 (99.8)	120 (99.5)	209 (99.2)	205 (99.2)	265 (99.0)	185 (99.3)	1,036 (96.3)	907 (96.7)
USA-13-019349-KF267450										146 (99.4)	205 (99.2)	201 (99.2)	285 (98.9)	181 (99.3)	1,041 (96.2)	912 (96.7)
AH2012_KC210145											176 (99.3)	163 (99.4)	264 (99.0)	146 (99.4)	1,025 (96.3)	893 (96.8)
BJ-2011-1_JN825712												91 (99.6)	258 (99.0)	74 (99.7)	989 (96.4)	859 (96.9)
GD-B-JX088695													255 (99.0)	32 (99.8)	1,024 (96.3)	894 (96.8)
CH-ZMDZY-11_KC196276														239 (99.1)	1,036 (96.3)	906 (96.7)
JS-HZ2012-KC210147															1,006 (96.4)	876 (96.8)
SM98_GU937797																148 (99.4)

[a] Due to space limits, only comparison results of 17 PEDV strains are shown here. All of the 10 U.S. PEDV strains are included. Among the 23 PEDV strains collected outside the United States, the 7 strains with lowest and highest nucleotide identities to U.S. PEDV strains are shown. The other 16 strains having nucleotide identities of 96.4% to 98.9% compared to the U.S. PEDV strains are not shown. Nucleotide differences and nucleotide identities between the viruses were determined at the whole-genome level.

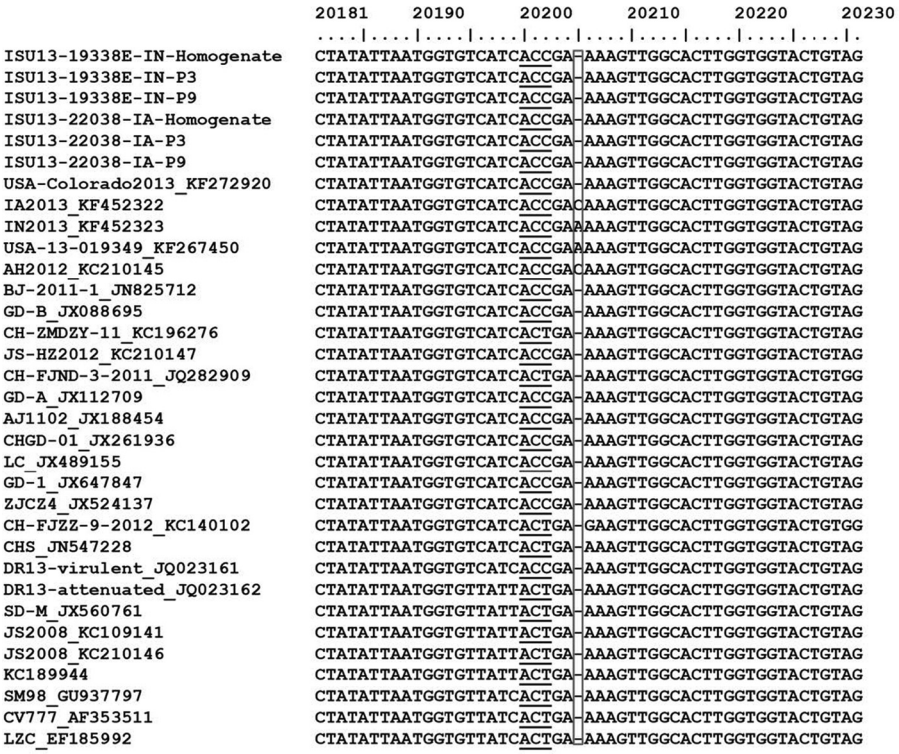

FIG 3 Alignment of partial ORF1b nucleotide sequences of 33 PEDV strains with entire genome sequences available. A single-nucleotide insertion between positions 20,204 and 20,205 of some PEDV strains is shown. The amino acid codon immediately before the insertion is shown as underlined.

aa). For both virus isolates, the mutations acquired at P3 were sustained through P9 (Table 2).

Sequence comparisons with other PEDV strains. The entire genome sequences of the six PEDV viruses examined in this study were compared to those of four other U.S. PEDV strains (sequenced from fecal samples) and 23 non-U.S. PEDV strains with entire genome sequences available in GenBank. All of the 10 U.S. PEDV strains were genetically closely related to each other (99.7% to 99.9% nucleotide identity) and differed from each other by 1 to 55 nucleotides at the whole-genome level (Table 3). The nucleotide identities and numbers of nucleotide differences between the U.S. PEDV strains and 23 non-U.S. PEDV strains ranged from 96.3% (differences of 1,022 to 1,041 nucleotides compared to the SM98-GU937797 strain) to 99.5% (differences of 118 to 146 nucleotides compared to the AH2012-KC210145 strain) (Table 3).

Alignment of the 10 U.S. PEDV strains identified a single nucleotide insertion (C or A) between nucleotides 20204 and 20205 in three strains, IA2013_KF452322 (22), IN2013_KF452323 (22), and USA-13-019349_KF267450 (27), compared to the six PEDV sequences determined in this study as well as to the USA/Colorado/2013_KF272920 strain sequence (Fig. 3). When the other 23 non-U.S. PEDV strains were included for comparison, it was found that only the AH2012_KC210145 strain had such an insertion and the other 22 strains did not (Fig. 3). Without such an insertion, the pp1ab protein of U.S. PEDV is predicted to be 6,782 aa in length. With such a frame-shifting insertion, the pp1ab protein of U.S. PEDV is predicted to stop earlier and be 6,649 aa in length. Since the entire genome sequences of all 10 U.S. PEDV viruses were determined by next-generation sequencing technology, the ORF1b portions (nucleotides 19923 to 20600) covering this insertion site were also sequenced using the traditional Sanger sequencing method for six PEDV (ISU13-19338E homogenate, P3, and P9 and ISU13-22038 homogenate, P3, and P9) for confirmation. None of the six PEDV sequences had such an insertion at that position.

Phylogenetic analysis of PEDV. A total of 33 PEDV viruses (6 determined in this study, 4 other U.S. PEDV strains, and 23 non-U.S. PEDV strains) were used for phylogenetic analysis based on different genes. Phylogenetic analysis based on the entire genome sequences demonstrated that 33 PEDV viruses can be clustered into group I and group II; each of the groups can be further divided into subgroups Ia, Ib, IIa, and IIb. The U.S. PEDV strains all clustered within subgroup IIa together with the AH2012_KC210145 strain that was detected in China in 2012 (Fig. 4 ["Entire genome"]). The phylogenetic trees based on the S gene, S1 portion, and S2 portion collectively demonstrated the same grouping structure as the tree based on the entire genome except as follows: (i) on the basis of the S, S1, and S2 trees, the U.S. PEDV strains were most closely related to strain CH-ZMDZY-11_KC instead of strain AH2012_KC210145 and (ii) strains DR-13-virulent_JQ023161 and CH-FJND-3-2011_JQ282909 clustered differently in the trees of S, S1, and S2 compared to the entire genome tree. The S1 and S2 trees were very similar to the S tree. The ORF3 tree also formed clusters I and II, but the structures were different from those of the other trees. The E tree included clusters I and II, but there were no clear subgroups in cluster II. The clusters formed in the M and N trees were similar to those in the trees based on the entire genome, S, S1, and S2; however, almost all virus strains in subgroup IIa of the M and N trees were

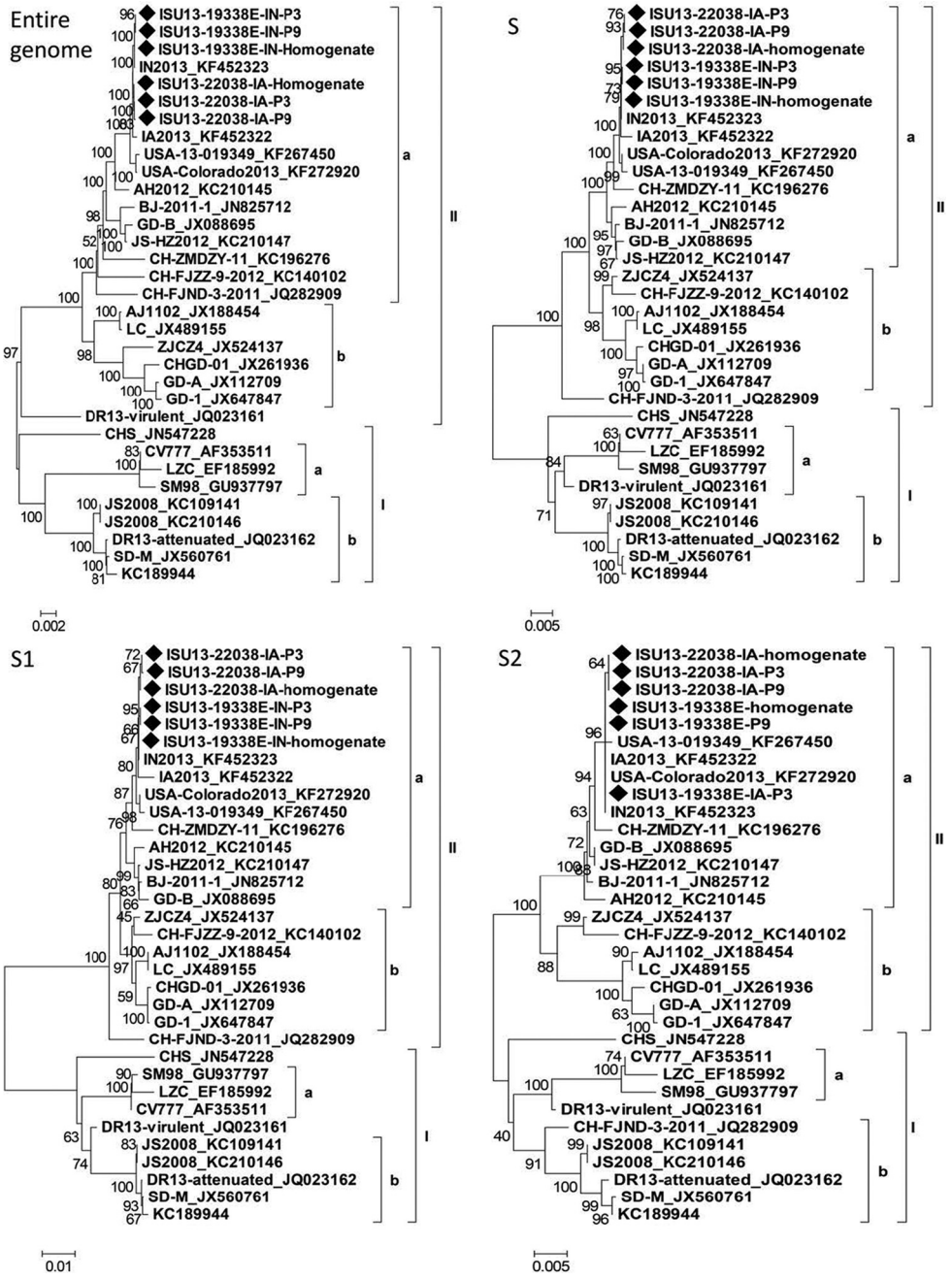

FIG 4 Phylogenetic analysis of the full-length genome, S gene, S1 portion, S2 portion, ORF3, E, M, and N gene nucleotide sequences of 6 U.S. PEDV from this study and 27 previously published PEDV sequences (GenBank numbers are shown in the figure). The trees were constructed using the distance-based neighbor-joining method of the software MEGA5.2. Bootstrap analysis was carried out on 1,000 replicate data sets, and values are indicated adjacent to the branching points. The viruses identified in this study are indicated by diamonds. Bar, 0.002 nucleotide substitutions per site.

equally genetically related to each other, which was not the case with the entire genome, S, S1, and S2 trees.

DISCUSSION

After PEDV was identified in the United States for the first time (22), endeavors to isolate a PEDV that can efficiently grow and propagate in cell culture were initiated. We attempted PED virus isolation (VI) from 33 feces samples and 17 intestine homogenates, and only 2 isolates were obtained (success rate, 4%). None of the VI attempts from feces were successful. Although the sample quality could have been a contributing factor to the low success rate, the isolation procedures also need to be further improved to increase the success rate of PEDV VI, particularly from fecal samples. The two isolates were serially propagated in cell culture and characterized. By examining the CPE development, immunofluorescence staining, EM, infectious virus titers, and entire genome sequences, we clearly demonstrated that the two PEDV isolates are phenotypically (titers, growth characteristics) and genetically sta-

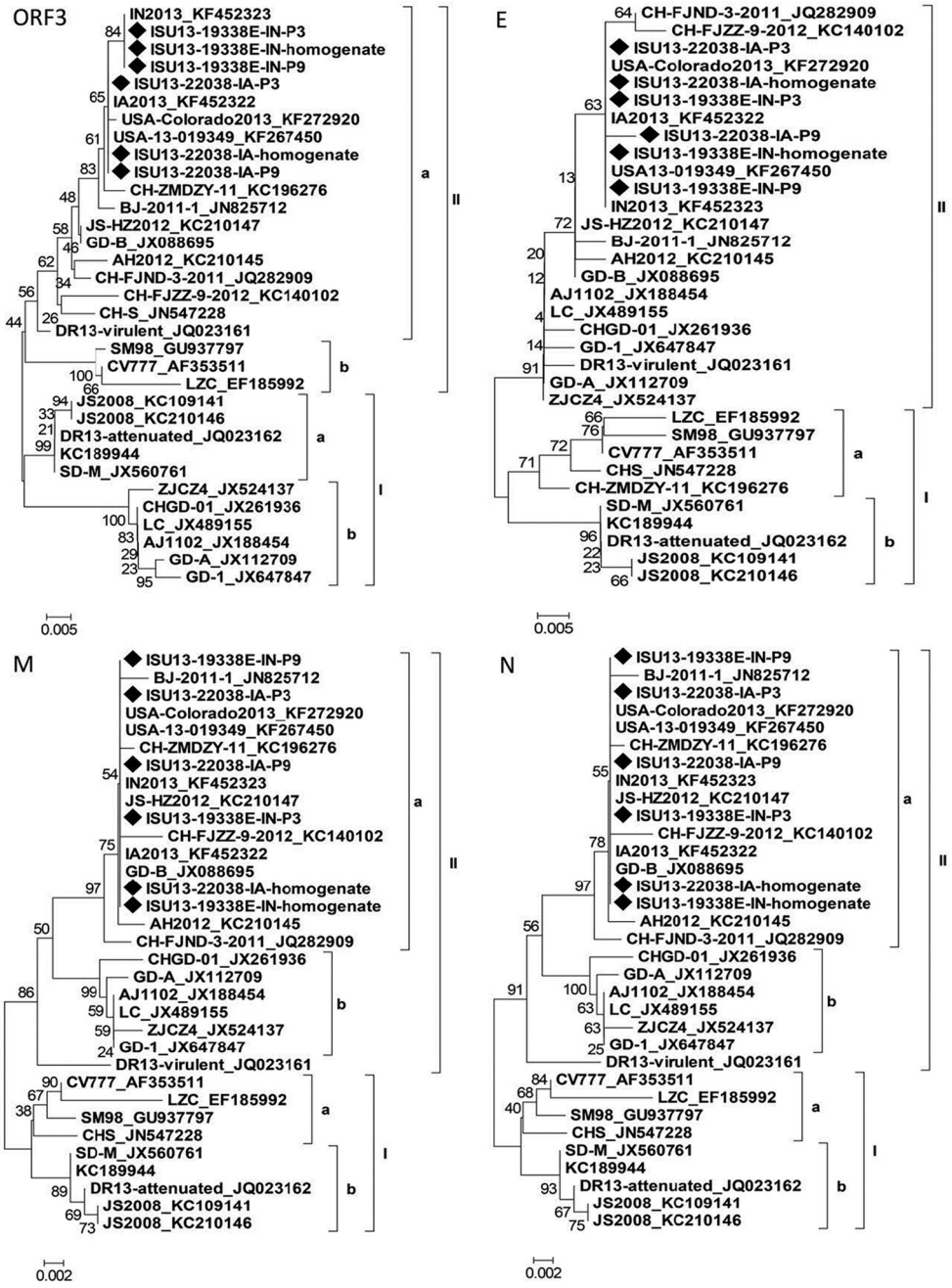

FIG 4 continued

ble during at least the first 10 serial passages in cell culture. Availability of the U.S. PEDV isolates provides an important tool for PEDV pathogenesis investigation, virological and serological assay development, and vaccine development. In fact, our PEDV isolates have been used in developing a PEDV-specific IFA that is currently offered (September 2013) at ISU VDL to measure PEDV antibodies in serum. In this study, we characterized the two isolates for the first 10 passages, but we have serially passaged the two isolates in cell culture for over 30 passages thus far. In general, live attenuated virus vaccines tend to elicit protective immunity more efficiently than inactivated virus vaccines, subunit vaccines, or DNA vaccines. We are continuing serial passages of these viruses in efforts to develop a live attenuated PEDV vaccine that could potentially be used to vaccinate nursery pigs and pregnant sows to mitigate the negative impact caused by PEDV infection. Viruses at selected passages will be inoculated into pigs to evaluate their virulence/attenuation phenotypes so that the genetic changes potentially associated with virus attenuation can be identified.

Next-generation sequencing technology provides a powerful tool to determine entire genome sequences with shorter turnaround time and lower costs. We are aware of 10 U.S. PEDV strains (ISU13-19338E homogenate, P3, and P9, ISU22038 homogenate, P3, and P9, Colorado2013_KF272920, IA2013_KF452322, IN2013_KF452323, and USA-13-019349_KF267450) whose whole-genome sequences have

been determined, and all of these were completed using the NGS technology. Among 33 PEDV strains evaluated in this study, only IA2013_KF452322, IN2013_KF452323, USA-13-019349_KF267450, and AH2012_KC210145 had one nucleotide insertion between positions 20204 and 20205 whereas the remaining 29 strains did not have such an insertion (Fig. 3). When strain Colorado2013_KF272920, which does not have such an insertion, was used as the reference sequence to map and assemble the ISU13-19338E and ISU13-22038 sequences, the resultant sequences did not have such an insertion. When the AH2012_KC210145, which has such an insertion, was used as the reference to map and assemble the sequences, surprisingly, the resultant sequences included such an insertion. In order to resolve the discrepancy and confirm the true status of the strains, the ISU13-19338E and ISU13-22038 viruses were sequenced for a portion covering the insertion site using the Sanger sequencing method. It was confirmed that such an insertion was not present in the ISU13-19338E and ISU13-22038 viruses. NGS technology has been increasingly used in research and diagnostic laboratories in recent years. However, bioinformatics analysis of NGS data is still a challenge for most laboratories. *De novo* assembly and analysis are time-consuming. For known viruses, a reference sequence is often used to map the NGS sequence data. It would be prudent to analyze the NGS data using two or more reference sequences and confirm any discrepancies by the Sanger method.

Based on sequence comparison and phylogenetic analysis, it appears that the U.S. PEDV strains are genetically closely related to some PEDV strains that were circulating in China in 2011 to 2012. However, it remains unknown how PEDV was introduced into the United States (22). The 10 U.S. PEDV viruses examined in this study are genetically closely related to each other, with 99.7% to 99.9% nucleotide identities at the whole-genome level. With the elapse of time and spread of PEDV to more farms in more states, a molecular epidemiology study is now needed to investigate the genetic evolution of PEDV in U.S. swine spatially and temporally. We are currently in the process of performing such a study.

Swine practitioners, diagnosticians, and researchers frequently ask which gene(s) of PEDV is appropriate for sequencing to study the genetic relatedness of viruses. We found that the phylogenetic trees based on the full-length S gene, the S1 portion, the S2 portion, the M gene, or the N gene of 33 PEDV strains have cluster structures similar to those seen in the tree based on the entire genome sequences. But the M and N genes are relatively conserved, and various PEDV strains may cluster together without reflecting the true genetic differences exhibited at the whole-genome level (e.g., subgroup IIa of the M and N trees in Fig. 4). In contrast, the full-length S gene, the S1 portion, or the S2 portion appears to be able to reflect the genetic diversity observed at the whole-genome level. As with other coronavirus S proteins, the PEDV spike protein makes up the surface projections of the virion and functions as the virus attachment protein interacting with the cell receptor (29). In addition, neutralization epitopes have been found in the PEDV spike protein (30–32). The full-length S gene is adequate for sequencing and molecular analysis of PEDV. However, the full-length S gene is approximately 4.1 kb and it may be difficult to sequence as a routine diagnostic service. The S1 portion is approximately 2.2 kb in length, and the S2 portion is approximately 1.9 kb in length. Considering that the receptor binding sites and majority of the neutralization epitopes are located in the S1 portion, it would be more appropriate to utilize this region of the genome for sequencing and molecular analysis to determine the genetic relatedness of different PEDV viruses.

In summary, two PEDV isolates associated with the PED outbreak in U.S. swine have been obtained and characterized. To our knowledge, this is the first report describing the isolation and characterization of U.S. PEDV. The U.S. PEDV strains were genetically closely related to each other and to some strains reported in China during 2011 to 2012. The full-length S gene or the S1 portion is appropriate for sequencing to study the genetic relatedness and molecular epidemiology of PEDV.

ACKNOWLEDGMENTS

We thank many swine veterinarians for submitting the clinical samples to the Iowa State University Veterinary Diagnostic Laboratory for PEDV investigation that made it possible for us to have access to the clinical materials for attempting PEDV isolation.

This study was supported by the Iowa State University Veterinary Diagnostic Laboratory and J.Z.'s start-up fund. Q.C. was partially supported by a fellowship sponsored by Zoetis.

REFERENCES

1. **Oldham J.** 1972. Letter to the editor. Pig Farming **1972**(October suppl): 72–73.
2. **Pensaert MB, de Bouck P.** 1978. A new coronavirus-like particle associated with diarrhea in swine. Arch. Virol. **58:**243–247. http://dx.doi.org/10.1007/BF01317606.
3. **Chasey D, Cartwright SF.** 1978. Virus-like particles associated with porcine epidemic diarrhoea. Res. Vet. Sci. **25:**255–256.
4. **International Committee on Taxonomy of Viruses.** 2012. Virus taxonomy: 2012 release. http://ictvonline.org/virusTaxonomy.asp?version=2012.
5. **Song D, Park B.** 2012. Porcine epidemic diarrhoea virus: a comprehensive review of molecular epidemiology, diagnosis, and vaccines. Virus Genes **44:**167–175. http://dx.doi.org/10.1007/s11262-012-0713-1.
6. **Ziebuhr J.** 2005. The coronavirus replicase. Curr. Top. Microbiol. Immunol. **287:**57–94. http://dx.doi.org/10.1007/3-540-26765-4_3.
7. **Van Reeth K, Pensaert M.** 1994. Prevalence of infections with enzootic respiratory and enteric viruses in feeder pigs entering fattening herds. Vet. Rec. **135:**594–597.
8. **Nagy B, Nagy G, Meder M, Mocsari E.** 1996. Enterotoxigenic Escherichia coli, rotavirus, porcine epidemic diarrhoea virus, adenovirus and calici-like virus in porcine postweaning diarrhoea in Hungary. Acta Vet. Hung. **44:**9–19.
9. **Martelli P, Lavazza A, Nigrelli AD, Merialdi G, Alborali LG, Pensaert MB.** 2008. Epidemic of diarrhoea caused by porcine epidemic diarrhoea virus in Italy. Vet. Rec. **162:**307–310. http://dx.doi.org/10.1136/vr.162.10.307.
10. **Takahashi K, Okada K, Ohshima K.** 1983. An outbreak of swine diarrhea of a new-type associated with coronavirus-like particles in Japan. Nihon Juigaku Zasshi **45:**829–832. http://dx.doi.org/10.1292/jvms1939.45.829.
11. **Kweon CH, Kwon BJ, Jung TS, Kee YJ, Hur DH, Hwang EK, Rhee JC, An SH.** 1993. Isolation of porcine epidemic diarrhea virus (PEDV) infection in Korea. Korean J. Vet. Res. **33:**249–254.
12. **Cheng Q.** 1992. Investigation on epidemic diarrhea in pigs in Qinghai region. Qinghai Xumu Shaoyi Zazhi **22:**22–23.
13. **Xuan H, Xing D, Wang D, Zhu W, Zhao F, Gong H.** 1984. Study on the culture of porcine epidemic diarrhea virus adapted to fetal porcine intestine primary cell monolayer. Chin. J. Vet. Sci. **4:**202–208.
14. **Puranaveja S, Poolperm P, Lertwatcharasarakul P, Kesdaengsakonwut S, Boonsoongnern A, Urairong K, Kitikoon P, Choojai P, Kedkovid R, Teankum K, Thanawongnuwech R.** 2009. Chinese-like strain of porcine epidemic diarrhea virus, Thailand. Emerg. Infect. Dis. **15:**1112–1115. http://dx.doi.org/10.3201/eid1507.081256.
15. **Chen J, Wang C, Shi H, Qiu H, Liu S, Chen X, Zhang Z, Feng L.** 2010. Molecular epidemiology of porcine epidemic diarrhea virus in China. Arch. Virol. **155:**1471–1476. http://dx.doi.org/10.1007/s00705-010-0720-2.
16. **Chen X, Yang J, Yu F, Ge J, Lin T, Song T.** 2012. Molecular characterization and phylogenetic analysis of porcine epidemic diarrhea virus (PEDV) samples from field cases in Fujian, China. Virus Genes **45:**499–507. http://dx.doi.org/10.1007/s11262-012-0794-x.

17. **Li Z, Chen F, Yuan Y, Zeng X, Wei Z, Zhu L, Sun B, Xie Q, Cao Y, Xue C, Ma J, Bee Y.** 2013. Sequence and phylogenetic analysis of nucleocapsid genes of porcine epidemic diarrhea virus (PEDV) strains in China. Arch. Virol. **158:**1267–1273. http://dx.doi.org/10.1007/s00705-012-1592-4.
18. **Li W, Li H, Liu Y, Pan Y, Deng F, Song Y, Tang X, He Q.** 2012. New variants of porcine epidemic diarrhea virus, China, 2011. Emerg. Infect. Dis. **18:**1350–1353. http://dx.doi.org/10.3201/eid1808.120002.
19. **Li ZL, Zhu L, Ma JY, Zhou QF, Song YH, Sun BL, Chen RA, Xie QM, Bee YZ.** 2012. Molecular characterization and phylogenetic analysis of porcine epidemic diarrhea virus (PEDV) field strains in south China. Virus Genes **45:**181–185. http://dx.doi.org/10.1007/s11262-012-0735-8.
20. **Fan JH, Zuo YZ, Li JH, Pei LH.** 2012. Heterogeneity in membrane protein genes of porcine epidemic diarrhea viruses isolated in China. Virus Genes **45:**113–117. http://dx.doi.org/10.1007/s11262-012-0755-4.
21. **Sun RQ, Cai RJ, Chen YQ, Liang PS, Chen DK, Song CX.** 2012. Outbreak of porcine epidemic diarrhea in suckling piglets, China. Emerg. Infect. Dis. **18:**161–163. http://dx.doi.org/10.3201/eid1801.111259.
22. **Stevenson GW, Hoang H, Schwartz KJ, Burrough ER, Sun D, Madson D, Cooper VL, Pillatzki A, Gauger P, Schmitt BJ, Koster LG, Killian ML, Yoon KJ.** 2013. Emergence of Porcine epidemic diarrhea virus in the United States: clinical signs, lesions, and viral genomic sequences. J. Vet. Diagn. Invest. **25:**649–654. http://dx.doi.org/10.1177/1040638713501675.
23. **Kim SH, Kim IJ, Pyo HM, Tark DS, Song JY, Hyun BH.** 2007. Multiplex real-time RT-PCR for the simultaneous detection and quantification of transmissible gastroenteritis virus and porcine epidemic diarrhea virus. J. Virol. Methods **146:**172–177. http://dx.doi.org/10.1016/j.jviromet.2007.06.021.
24. **Hofmann M, Wyler R.** 1988. Propagation of the virus of porcine epidemic diarrhea in cell culture. J. Clin. Microbiol. **26:**2235–2239.
25. **Reed LJ, Muench H.** 1938. A simple method of estimating fifty percent endpoints. Am. J. Hyg. (Lond) **27:**493–497.
26. **Doane FW, Anderson N.** 1987. Electron microscopy in diagnostic virology: a practical guide and atlas. Cambridge University Press, Cambridge, United Kingdom.
27. **Marthaler D, Jiang Y, Otterson T, Goyal S, Rossow K, Collins J.** 2013. Complete genome sequence of porcine epidemic diarrhea virus strain USA/Colorado/2013 from the United States. Genome Announc. **1:**e00555–13. http://dx.doi.org/10.1128/genomeA.00555-13.
28. **Lee DK, Park CK, Kim SH, Lee C.** 2010. Heterogeneity in spike protein genes of porcine epidemic diarrhea viruses isolated in Korea. Virus Res. **149:**175–182. http://dx.doi.org/10.1016/j.virusres.2010.01.015.
29. **Bosch BJ, van der Zee R, de Haan CA, Rottier PJ.** 2003. The coronavirus spike protein is a class I virus fusion protein: structural and functional characterization of the fusion core complex. J. Virol. **77:**8801–8811. http://dx.doi.org/10.1128/JVI.77.16.8801-8811.2003.
30. **Chang SH, Bae JL, Kang TJ, Kim J, Chung GH, Lim CW, Laude H, Yang MS, Jang YS.** 2002. Identification of the epitope region capable of inducing neutralizing antibodies against the porcine epidemic diarrhea virus. Mol. Cells **14:**295–299.
31. **Cruz DJ, Kim CJ, Shin HJ.** 2008. The GPRLQPY motif located at the carboxy-terminal of the spike protein induces antibodies that neutralize Porcine epidemic diarrhea virus. Virus Res. **132:**192–196. http://dx.doi.org/10.1016/j.virusres.2007.10.015.
32. **Sun D, Feng L, Shi H, Chen J, Cui X, Chen H, Liu S, Tong Y, Wang Y, Tong G.** 2008. Identification of two novel B cell epitopes on porcine epidemic diarrhea virus spike protein. Vet. Microbiol. **131:**73–81. http://dx.doi.org/10.1016/j.vetmic.2008.02.022.